PHYSICAL REVIEW A VOLUME 53, NUMBER 4 APRIL 1996

Anomalous resonance fluorescence from an atom in a cavity with injected squeezed vacuum

W. S. Smyth and S. Swain*
Department of Applied Mathematics and Theoretical Physics, The Queen's University of Belfast, Belfast BT7 1NN, Northern Ireland
(Received 28 August 1995)

As a realistic system for observing the distinctive features of the interaction of squeezed light with atoms, we consider a single, coherently driven, two-level atom in a resonant optical cavity coupled to a broadband squeezed vacuum field. In the bad cavity limit we derive equations of motion for the atomic operators that are identical to those for the free-space situation, except for having modified parameters. We focus our attention on the resonance fluorescence from this system and show that, in the above limit, many of the unusual spectral features previously reported for the free atom situation persist. We also confirm the link between these anomalous spectra and the collapse of an atom into a pure state. The cavity parameter values needed to verify some of these interesting effects appear to be within the range of present day technology.
PACS number(s): 42.50.Dv, 32.80.−t

I. INTRODUCTION

The phenomenon of resonance fluorescence constitutes a central problem in quantum optics. It is an aspect of matter-radiation interaction that has been extensively considered over the years. As early as the 1930s Weisskopf used a quantum perturbation approach to describe weak-field resonance fluorescence from free atoms [1]. More recently Mollow showed that the resonance fluorescence spectra from a strongly driven atom had a three-peaked structure [2], which was subsequently observed [3]. He predicted the central peak of the incoherent spectrum to have a width equal to the natural spontaneous decay rate of the atom while each of the sidebands are one and a half times as broad. Photon antibunching and squeezing have been predicted in resonance fluorescence, but so far only antibunching has been observed [4].

The squeezing of light fields is another major area of interest [5]. Radiation fields of this nature find their roots in the foundations of quantum mechanics itself. That quantum fluctuations can, in one field quadrature, exhibit less noise than empty space without violating the uncertainty principle, not only has implications at a fundamental level but also potential applications in areas such as telecommunications [6] and high precision measurement, e.g., in the detection of gravity waves [7]. The signal from such a field would, with standard interferometry techniques, be swamped by the noise from the normal vacuum. Squeezed light has also been used to enhance sensitivity in saturation spectroscopy [8].

A decade after the first experimental demonstration of squeezed light generation [9], we have arrived at the stage where many laboratories can successfully produce squeezed sources. This has provided extra impetus to the search for novel features in the interaction of squeezed light with atomic systems.

The first prediction of fundamentally different behavior was made by Gardiner [10] who showed that the two quadratures of the polarization of a two-level atom damped via its interaction with a broadband squeezed vacuum decay at vastly different rates. The modifications to the resonance fluorescence spectra of such a system were considered by Carmichael, Lane, and Walls [11]. They found that for weak driving fields the linewidth of the spectra could be drastically reduced, ultimately vanishing in the limit of arbitrarily strong squeezing. They also showed that for large classical applied field strengths the spectrum became a triplet, as in the absence of squeezing [2], but that the height and width of the central peak of the triplet depended strongly on the relative phase of the squeezed and driving fields.

As Gardiner and Carmichael, Lane, and Walls indicated, these effects would be difficult to realize experimentally in the free-space situations considered since they required the squeezed modes to occupy the whole 4π solid angle. It was therefore necessary to consider alternative systems that relaxed this condition while still enabling the desired effects to be observable. The cavity situation is a natural one to consider. When an atom is placed between mirrors or inside an optical cavity it interacts with a modified electromagnetic vacuum. Many features of this modified system have been verified including cavity-enhanced and inhibited spontaneous emission [12]. In the good coupling limit, vacuum Rabi splitting has been predicted [13] and observed [14], with of the order of one atom in the cavity at a time. This system exhibits many other interesting features, and an increasing number have been subjected to experiment. One reason for the advance in experimental work is recent developments in atomic beam and atomic trapping techniques.

Parkins and Gardiner [15] have considered a single atom inside a microcavity that has squeezed light incident upon the output mirror. They show that the inhibition of atomic phase decays can still be observed under appropriate phase matching conditions.

The aspect of squeezed-light–atom interactions that interests us here is that of resonance fluorescence. Specifically we are concerned with the ''anomalous'' resonance fluorescence spectra [16–18]. These have been discussed for the free-space situation, but experiments to demonstrate these effects are likely to take place within the cavity environment. Our particular aim is to show that many of these free-space properties do in fact carry over to a measurable extent to the cavity configuration.

*Also at the Department of Physics, The University of Queensland, Brisbane, Queensland 4072, Australia.

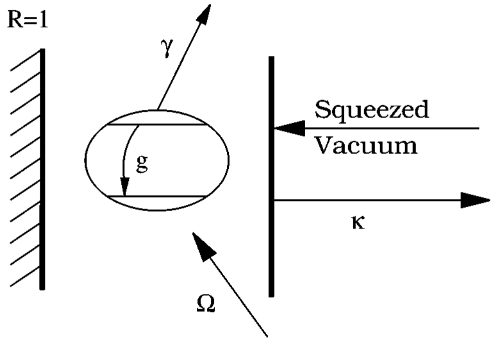

FIG. 1. A schematic representation of the physical system under consideration.

A number of papers have examined the conditions for the existence of pure states in systems of interacting atoms and fields. We are particularly concerned with the situation where an applied squeezed field is present. Palma and Knight [19] showed that a pair of two-level atoms in the presence of a squeezed field but in the absence of a classical driving field may collapse into a pure state. The corresponding three-level system was considered by Buzek, Knight, and Kudryavtsev [27]. Agarwal and Puri [20] considered a number of two-level atoms driven by a classical field in the presence of a squeezed vacuum and showed that, under appropriate circumstances, the atomic system may evolve into a pure state. The single-atom version of this system was further considered by Tucci [21], who emphasized the statistical mechanical aspects. We showed that, for large N, the appearance of the anomalous resonance fluorescence spectra coincides with the state of the system being a pure one [18].

It has also been pointed out that a number of atoms interacting with a driving field in the cavity environment (but with no applied squeezed vacuum) can also evolve into a pure state [22,23]. Such systems also exhibit nonclassical features in their output. In this situation, however, it is a pure state of the combined atom-field system, rather than the atom alone, which is involved.

The structure of the rest of this paper is as follows: the physical system under consideration is described in Sec. II, where we also derive the equations of motion in the bad cavity limit. We show that these are formally identical to those in free-space, the only difference being a redefinition of parameters. In Sec. III we investigate the anomalous resonance fluorescence spectra for this system, and we determine how well the steady state of the atom in these cases can be approximated by a pure state. We compare this situation with that for the free-space environment. Section IV contains our conclusions.

II. THE TWO-LEVEL ATOM IN THE BAD CAVITY LIMIT

We consider a single two-level atom, coupled to a resonant cavity mode, and coherently driven through the open sides of this single-ended cavity. (See Fig. 1.) A broadband squeezed vacuum also interacts with this system. The Bohr frequency of the atom, the cavity resonance frequency, and the center frequency of the squeezed vacuum are all taken to be identical.

In a frame rotating at the resonance frequency the master equation is

$$\dot{\rho}=i[H,\rho]+\gamma L_a\rho+\kappa L_c\rho, \tag{1}$$

where H is given by the sum of the driving and Jaynes-Cummings Hamiltonians,

$$H_d=\tfrac{1}{2}\Omega(\sigma_-+\sigma_+) \quad \text{and} \quad H_{\rm JC}=ig(\sigma_+a-\sigma_-a^\dagger), \tag{2}$$

with

$$L_a\rho=2\sigma_-\rho\sigma_+-\sigma_+\sigma_-\rho-\rho\sigma_+\sigma_- \tag{3}$$

and

$$\begin{aligned} L_c\rho=&(N+1)(2a\rho a^\dagger-a^\dagger a\rho-\rho a^\dagger a)\\ &+N(2a^\dagger\rho a-aa^\dagger\rho-\rho aa^\dagger) \qquad (4)\\ &-M[\exp(-i\phi_v)(2a\rho a-a^2\rho-\rho a^2)+\text{H.c.}]. \qquad (5)\end{aligned}$$

$L_a\rho$ and $L_c\rho$ describe atomic damping to modes other than the privileged cavity mode, and damping of the cavity field by the squeezed reservoir, respectively. The cavity mode has the annihilation and creation operators a and $a^\dagger$ while the atom is represented by the usual Pauli spin-$\frac{1}{2}$ operators σ_+ , σ_- , Ω is the Rabi frequency of the driving laser field, g is a measure of the atom-cavity coupling, and γ and κ are the atomic and cavity decay constants, respectively.

The broadband squeezed reservoir is characterized by the real parameters N and M through the relations [5]

$$\langle a^\dagger(\omega_1)a(\omega_2)\rangle=N\delta(\omega_1-\omega_2), \tag{6}$$

$$\langle a(\omega_1)a(\omega_2)\rangle=M\exp(i\phi_v)\delta(\omega_1+\omega_2), \tag{7}$$

where $a(\omega)$ creates a photon of the squeezed vacuum with frequency ω. Another important parameter is the squeezing phase, defined as

$$\Phi=2\phi_L-\phi_v=-\phi_v\,, \tag{8}$$

where ϕ_L is the laser phase, which is taken to be zero in Eq. (2) above. The squeezed vacuum contains real photons with N the mean number of photons present (over all frequencies), and M the magnitude of the two-photon correlations. It is the latter that provides the essential nonclassical features of the squeezing process. For a given squeezing photon number N, M is bounded above by its value for a minimum uncertainty state. It is convenient here to introduce the parameter η where $0\leqslant\eta\leqslant1$, which enables us to write

$$M=\eta[N(N+1)]^{1/2}. \tag{9}$$

The quantity η measures the degree of two-photon correlations in the squeezed vacuum. Its interpretation is simple: $\eta=0$ implies no squeezing and our cavity field is then equivalently damped by a chaotic field. $\eta=1$ on the other hand corresponds to the reservoir being in an ideal squeezed state or minimum uncertainty squeezed state. We refer to this as perfect correlation, since in this instance the photon twins, so typical of a squeezed vacuum, are maximally correlated for the particular value of N.

The atomic operators mentioned above satisfy the commutation relations $[\sigma_+,\sigma_-]=2\sigma_z$, $[\sigma_z,\sigma_\pm]=\pm\sigma_z$. Using these relations and (1) we can derive the time evolution of the expectation values of these operators:

$$\langle\dot{\sigma}_-\rangle=-\gamma\langle\sigma_-\rangle+2g\langle\sigma_z a\rangle-i\Omega\langle\sigma_z\rangle,$$

$$\langle\dot{\sigma}_+\rangle=-\gamma\langle\sigma_+\rangle+2g\langle\sigma_z a^\dagger\rangle+i\Omega\langle\sigma_z\rangle, \tag{10}$$

$$\langle\dot{\sigma}_z\rangle=-\gamma(2\langle\sigma_z\rangle+1)-g(\langle a^\dagger\sigma_-\rangle+\langle a\sigma_+\rangle)$$
$$+i\tfrac{1}{2}\Omega(\langle\sigma_+\rangle-\langle\sigma_-\rangle).$$

These equations contain higher-order operator expectation values. This leads to a series of coupled equations that must be solved to leave evolution equations in the atomic operators only. We now adopt the approach used by Rice and Pedrotti [24]. They showed that in the bad cavity limit (see below) this hierarchy of equations can be truncated to yield the following:

$$\langle\dot{\sigma}_-\rangle=-\gamma[1+C(2N+1)]\langle\sigma_-\rangle-2CM\gamma\exp(i\Phi)\langle\sigma_+\rangle$$
$$-i\Omega\langle\sigma_z\rangle,$$

$$\langle\dot{\sigma}_+\rangle=-\gamma[1+C(2N+1)]\langle\sigma_+\rangle-2CM\gamma\exp(-i\Phi)\langle\sigma_-\rangle$$
$$+i\Omega\langle\sigma_z\rangle, \tag{11}$$

$$\langle\dot{\sigma}_z\rangle=-2\gamma[1+C(2N+1)]\langle\sigma_z\rangle+i\tfrac{1}{2}\Omega(\langle\sigma_+\rangle-\langle\sigma_-\rangle)$$
$$-2\gamma(1+C).$$

The parameter $C=g^2/\kappa\gamma$ is the single-atom cooperativity parameter familiar from optical bistability.[1] The validity of the truncation depends on the relative sizes of the various systematic parameters. Thus we can define the bad cavity limit as [23]

$$\kappa\gg\Omega,g,\gamma \quad \text{with} \quad g\gg\gamma \quad \text{and} \quad C=g^2/\kappa\gamma \text{ finite.} \tag{12}$$

In contrast to Rice and Pedrotti we chose to drive the atom directly but the physics contained in both approaches is the same [25]. Also, to ensure the validity of the broadband squeezing assumption, the bandwidth of squeezing would need to be large compared to κ.

There is clearly a link between Eqs. (11) and the standard free-space Bloch equations for the equivalent system, but for a more direct comparison with the free-space analysis we express these equations in terms of the atomic density matrix elements. Using the relation $\langle A\rangle=\mathrm{Tr}(\rho A)$ and the cyclic properties of the trace (Tr) we have

$$\dot{\rho}_{00}=-2CN\gamma\rho_{00}+2\gamma[(1+C)+CN]\rho_{11}-i\tfrac{1}{2}\Omega(\rho_{10}-\rho_{01}),$$

$$\dot{\rho}_{11}=-2\gamma[(1+C)+CN]\rho_{11}+2CN\gamma\rho_{00}+i\tfrac{1}{2}\Omega(\rho_{10}-\rho_{01}), \tag{13}$$

$$\dot{\rho}_{01}=-[(1+C)+2CN]\gamma\rho_{01}-2CM\gamma\exp(i\Phi)\rho_{10}$$
$$-i\tfrac{1}{2}\Omega(\rho_{11}-\rho_{00}),$$

$$\dot{\rho}_{10}=-[(1+C)+2CN]\gamma\rho_{10}-2CM\gamma\exp(-i\Phi)\rho_{01}$$
$$+i\tfrac{1}{2}\Omega(\rho_{11}-\rho_{00}).$$

Identifying $2CN\gamma$ with the incoherent transition rate from ground to excited state (γ_{01}) and $2\gamma[(1+C)+CN]$ as the rate for the incoherent processes in the opposite direction (γ_{10}), we note that physical considerations require them to differ only by spontaneous emission.

Thus we can write

$$\gamma_{01}=4CN\gamma=2\gamma(1+C)\frac{C}{1+C}2N$$

and

$$\gamma_{10}=2\gamma[(1+C)+CN]=2\gamma(1+C)\left(1+\frac{C}{1+C}N\right),$$

so that defining

$$\gamma_c=(1+C)\gamma,$$

$$N_c=\frac{C}{1+C}N, \tag{14}$$

$$M_c=\frac{C}{1+C}M,$$

we have

$$\gamma_{01}=2N_c\gamma_c \text{ and } \gamma_{10}=2(N_c+1)\gamma_c, \tag{15}$$

where γ_c is the cavity enhanced spontaneous emission rate.

The factor $C/(1+C)$ that appears in the above expressions has the following interpretation. γ is the rate of spontaneous decay into the noncavity modes, and $\gamma_c=\gamma(1+C)$ is the total spontaneous emission rate, so that $C\gamma$ is the cavity enhanced contribution. The factor $C/(1+C)$ is therefore the ratio of the spontaneous emission into the cavity mode to the total spontaneous decay rate. This quantity is sometimes referred to as the *beta value* of the cavity system. The atom therefore experiences an effective squeezed field whose parameters are modified by the beta factor.

Thus making the appropriate changes throughout Eqs. (13) we have

$$\dot{\rho}_{00}=-\gamma_{01}\rho+\gamma_{10}\rho_{11}-i\tfrac{1}{2}\Omega(\rho_{10}-\rho_{01}),$$

$$\dot{\rho}_{11}=-\gamma_{10}\rho_{11}+\gamma_{01}\rho_{00}+i\tfrac{1}{2}\Omega(\rho_{10}-\rho_{01}), \tag{16}$$

$$\dot{\rho}_{01}=-\tfrac{1}{2}\gamma_s\rho_{01}-M_c\gamma_c\exp(i\Phi)\rho_{10}-i\tfrac{1}{2}\Omega(\rho_{11}-\rho_{00}),$$

$$\dot{\rho}_{10}=-\tfrac{1}{2}\gamma_s\rho_{10}-M_c\gamma_c\exp(-i\Phi)\rho_{01}+i\tfrac{1}{2}\Omega(\rho_{11}-\rho_{00}),$$

[1] Because of a factor of 2 difference in the definitions of γ, there is a numerical difference between our parameter C and that of Rice and Pedrotti. The present choice reduces the number of factors of 2 that appear in our expressions.

where $\gamma_s = \gamma_{01} + \gamma_{10}$.

Equations (16) are formally identical to the density matrix equations in free-space. Thus it would seem reasonable to assume that we could reproduce any of the previous results for the free atom. However, we already know from simple physical arguments that since the atom sees unsqueezed modes through the open sides of the cavity there is a limit to the amount of linewidth narrowing achievable in this model. This can be easily seen in the mathematics. If we transform Eqs. (11) by setting $\sigma_+ = \sigma_x + i\sigma_y$ and $\sigma_- = \sigma_x - i\sigma_y$ then from the equation for σ_x,

$$\langle \dot{\sigma}_x \rangle = -2\gamma[1 + C(1 + 2N - 2M\cos\Phi)]\langle \sigma_x \rangle - 2CM\gamma \sin\Phi \langle \sigma_y \rangle, \tag{17}$$

it is easily seen that only the cavity enhanced part of the decay rate is phase dependent, rather than the whole decay rate as would be the case for 4π solid angle squeezing.

Gardiner [10] showed that the basic difference in the decay of an atom bathed in squeezed modes rather than in a standard reservoir was that the two atomic polarization quadratures decayed at different rates, and that in the case of minimum uncertainty squeezing, one decay rate tended to zero for $N \to \infty$. Many results in the free-space situation were derived in this limit. One might then ask how it is that equations have been derived which, on the one hand, are formally identical to those for the free atom and yet on the other hand apply in a regime where arbitrarily large linewidth narrowing is not possible.

The answer is contained in the relation between N_c and M_c, the parameters defined in Eqs. (14). Notice that in Eqs. (16), we must now interpret N_c and M_c as the *effective* squeezing parameters experienced by the atom in the bad cavity limit. It is as though we were considering a driven free atom damped by a broadband squeezed vacuum but that the squeezing in the reservoir was now described by N_c and M_c. In the free-space case, the parameters N and M appearing in the master equation (1) are related as follows:

$$M \leqslant [N(N+1)]^{1/2}. \tag{18}$$

Now in the bad cavity limit we have instead

$$M_c = \frac{C}{1+C} M \leqslant \frac{C}{1+C}[N(N+1)]^{1/2} \tag{19}$$

$$\tag{20}$$

$$= \left[N_c \left(N_c + \frac{C}{1+C} \right) \right]^{1/2} < [N(N+1)]^{1/2}, \tag{21}$$

so that ultimately in this limit we cannot implement what would be perfectly correlated (minimum uncertainty) squeezing, i.e., the effective degree of correlation of the squeezing, in our model, is necessarily reduced from its value in the input squeezed field. Defining η_c as

$$\eta_c = \frac{M_c}{[N_c(N_c+1)]^{1/2}} \tag{22}$$

we have

$$0 \leqslant \eta_c < 1 \tag{23}$$

and using the relation (9) we can simply evaluate the unavoidable fractional modification as

$$\frac{\eta_c}{\eta} = \left[1 + \frac{1}{C(N+1)} \right]^{-1/2} \simeq 1 - \frac{1}{2C(N+1)} \quad \text{for } CN \gg 1. \tag{24}$$

By taking N or C large, we obtain $\eta_c \simeq \eta$. Even in these limits, however, the decay rate of the in-phase component of the polarization cannot be made arbitrarily narrow, as it can in free-space [10]: there is always the residual width of γ, the spontaneous decay rate into the unsqueezed modes. For large C, we also note that the unsqueezed linewidth $\gamma_c = \gamma(1+C)$ becomes very large. This quantity determines the scale of the spectral features.

Let us summarize the position to date. Having started from the master equation for the density operator we have, via an adiabatic elimination of the cavity field in the bad cavity limit, derived equations of motion for the density matrix elements that are identical to those for the free, driven atom, bathed in 4π solid angle broadband squeezing, but where these modes necessarily have less than perfect squeezing correlations.

With regard to resonance fluorescence, we may expect qualitatively similar spectra to those previously reported [16–18,26] but for the case of an imperfectly correlated squeezed vacuum. It is already clear that effects that are extremely sensitive to the degree of correlation of the squeezing will be difficult to reproduce, at least for experimentally feasible values of N and C. It should be noted that the sensitivity to the degree of correlation generally decreases with N [17].

III. THE RESONANCE FLUORESCENCE SPECTRA

We consider here only the incoherently scattered part of the resonance fluorescence spectrum. It is worth noting here that the fluorescence from our system is carried away via the normal vacuum modes, which exist out the sides of the cavity. This plays the role of the unsqueezed window implicit in the calculations of [10,11].

The spectrum is related to the Fourier transform of the atomic correlation function [26]

$$\Lambda(\omega) = \mathscr{R}\left[\int_0^\infty \langle \sigma_+(0)\sigma_-(\tau)\rangle e^{i(\omega-\omega_L)\tau} d\tau \right], \tag{25}$$

where $\mathscr{R}$ denotes the real part and the $\sigma_\pm$ are the Pauli spin-$\frac{1}{2}$ operators mentioned above. Working in Laplace space the evolution equations of these operators together with the quantum regression theorem may be used to calculate the spectrum. Specifically we have

$$\Lambda(\omega) = \mathscr{R}[F(z = -i\omega)], \tag{26}$$

where ω is the frequency measured from the atomic resonance frequency and [26]

$$F(z)=\frac{z[(z+2\Gamma)(z+\Gamma)+\frac{1}{2}\Omega^2]\rho+s(z+\gamma_c)[z+\Gamma+\gamma_c M_c e^{i\Phi}]}{z\{(z+2\Gamma)[(z+\Gamma)^2-\gamma_c^2 M_c^2]+\Omega^2(z+\Gamma+\gamma_c M_c\cos\Phi)\}},\tag{27}$$

with $\Gamma=\gamma_c(N_c+\frac{1}{2})$, and

$$\rho=\frac{\gamma_c N_c(\Gamma^2-\gamma_c^2 M_c^2)+\frac{1}{2}\Omega^2(\Gamma+\gamma_c M_c\cos\Phi)}{2\Gamma(\Gamma^2-\gamma_c^2 M_c^2)+\Omega^2(\Gamma+\gamma_c M_c\cos\Phi)},\tag{28}$$

$$s=\frac{\gamma_c\Omega^2(\frac{1}{2}\Gamma+\gamma_c M_c e^{i\Phi})}{2\Gamma(\Gamma^2-\gamma_c^2 M_c^2)+\Omega^2(\Gamma+\gamma_c M_c\cos\Phi)},\tag{29}$$

are related to the steady-state excited population and the atomic coherence, respectively.

In the free-space situation we are interested in the regime $\Omega\simeq\gamma_c$ where the Mollow sidebands are not resolved and the spectra normally consist of two components. The normal spectra [11] consist of a sharp (subnatural) line at line center superimposed upon a very broad, shallow background.

In recent publications [16–18] it was shown that under very restrictive conditions, dispersive profiles, quite unlike any previously reported for this system, could be found. It was also shown that anomalous spectra existed over a continuous but narrow range of parameter values. These spectra took on a variety of profiles including holes, pimples, and a vanishing of the central feature altogether. The presence of the squeezed vacuum was essential for these effects. The origin of these spectra together with a prescription of how to locate the parameter region of interest was given.

The prescription followed from a realization that when these anomalous features arose the normal contributions to the spectrum were greatly reduced in magnitude. Consequently we expect to find these spectra at those parameter values that minimize the incoherent part of the line-center amplitude $\Lambda_i(0)$.

Returning now to the cavity situation, we note that the features of the spectrum are determined by the poles and residues of (27). The poles are given approximately by

$$z_0=\frac{\gamma_c^2+8\Omega^2\cos^2\Phi/2}{\Gamma},$$

$$z_\pm=-\left(\Gamma-\frac{1}{2}z_0\right)\pm i\Omega\sin\Phi/2\tag{30}$$

in the regime of greatest interest, $\Phi\lesssim\pi/2$, $\Gamma\gg\gamma_c$, and $\Omega\simeq\gamma_c$. Since $z_0\ll\mathrm{Re}(z_\pm)$, the sharp features of the spectrum will result from z_0. The contribution from the poles at $z=z_\pm$ will be a flat, largely featureless background. Consequently, we concentrate on the contributions from the pole at $z=z_0$.

The incoherent part of the spectrum has the form

$$\Lambda_i(\omega)=\sum_{k=-1}^{+1}\frac{x_k\alpha_k-y_k(\omega-\beta_k)}{(\omega-\beta_k)^2+\alpha_k^2},\tag{31}$$

where $z_k=\alpha_k+i\beta_k$ are the poles, and the residues of the incoherent part of (27) are of the form $R_k=x_k+iy_k$ [16]. We find

$$x_0=\frac{(a-2)^2}{16a^2}-\frac{\frac{3}{4}(a^2-4)a+1}{4a^2\Gamma^2/\gamma_c^2},$$

$$y_0=\frac{\Omega^2\sin\Phi}{2a\Gamma^2},\quad a=1+\frac{4\Omega^2\cos^2\Phi/2}{\gamma_c^2}.\tag{32}$$

These expressions suggest that $\Lambda_i(0)$ will be a minimum when $a=2$, which gives

$$\Omega=\frac{\gamma_c}{2\cos\Phi/2},\tag{33}$$

which, with the replacement of γ by γ_c, gives the condition we have obtained previously for the free-space situation [16–18].

We adopt the same prescription here in searching for the anomalous spectra in our cavity configuration: we determine numerically the parameter values that minimize $\Lambda_i(0)$. However, we have the added complication of taking into account the parameter η_c. Recall that η_c now describes the effective degree of correlation of the squeezing as experienced by the atom and this consequently provides a further limiting factor to both the existence of the anomalous spectral profiles and to the robustness of any features that do exist.

From expression (24), η_c is determined from the degree of correlation present in the squeezed bath initially coupled into our system as well as by the strength N of the squeezing. It also depends on the value of C. For what follows we will assume that the squeezed vacuum injected into the cavity was perfectly correlated. Suppose that an anomalous feature existed in the free-space case for a particular value of the correlation coefficient—say $\eta=\eta_1$. Then, if we can achieve a sufficiently large value for η_c to satisfy $\eta_c\geqslant\eta_1$, we may continue in the knowledge that it will also exist in our cavity configuration.

Let us first consider the case of $\Phi=\pi/2$. It has been shown that, in the free-space situation, prominent dispersive features arise in the resonance fluorescence spectra for large N and $\Omega^2=1/2$, providing $\eta=1$ [16]. In Fig. 2 we show the spectra for the case where $N=10$ and $\Omega^2=1/2$, and initially $\eta=1$. The figure shows that if η is reduced by as little as 0.0005% from the value unity, then the dispersive profile vanishes. This implies that we need $\eta_c>0.999\,995$. Using (24) we see that to attain this value of η_c given $\eta=1$, $N=10$, we require $C\geqslant 5\times10^3$. Unfortunately this an order of magnitude greater than is currently experimentally achievable. In Fig. 2 we show the spectra for the above values of η and N and for four values of C. As expected the dispersive profiles are only apparent for extremely large values of C.

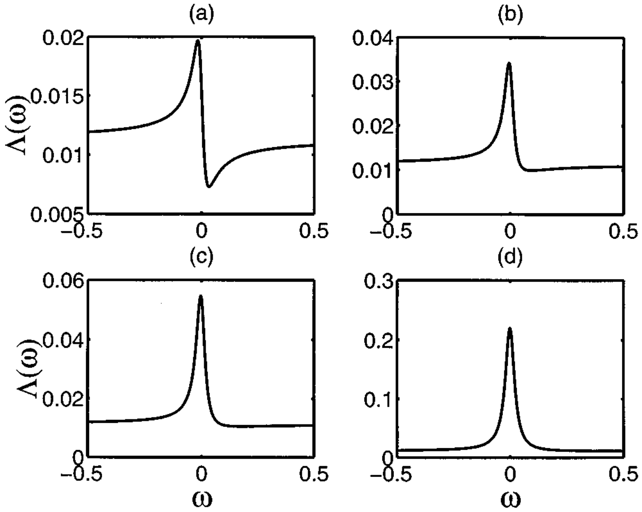

FIG. 2. The resonance fluorescence spectra in the bad cavity case, for $N=10$ and $C=5\times10^4$, 10^4, 5×10^3, and 10^3 for frames (a), (b), (c), and (d), respectively. In all our figures, we take $\gamma=1$, so that the Rabi frequency Ω and the fluorescence frequency ω are measured relative to this quantity. The value of Ω in each case has been taken to optimize the effect for the given value of C. [$\Omega=0.69$ in frames (a), (b), and (c); $\Omega=0.72$ in frame (d).] The corresponding values of η for the equivalent free-space situation are η=0.999 999 95, 0.999 998, 0.999 995, 0.999 98.

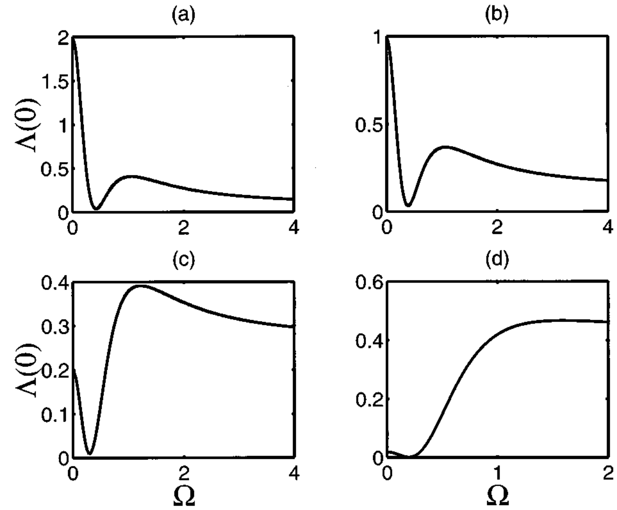

FIG. 4. The cavity resonance fluorescence intensity at line center $\Lambda(0)$ as a function of the Rabi frequency Ω . The phase is fixed at $\Phi=0$ throughout and (a) $N=1$, $C=200$, (b) $N=0.5$, $C=100$, (c) $N=0.1$, $C=50$, and (d) $N=0.01$, $C=10$.

We should emphasize that the sensitivity of the anomalous features to the value of η decreases as N decreases, so that in choosing the large value $N=10$ we have a particularly fragile situation, and one particularly difficult to test experimentally. If we reduce the value of N to $N=1$, for example, it may be shown that the dispersive profiles are still evident for $\eta=0.999$, which corresponds to $C\simeq125$. In Fig. 3 we plot the resonance fluorescence spectra for some smaller values of N and C. In frames (a) and (b), where $N=0.5$ and $C=125$ and 100, respectively, the dispersive nature of the spectra remains apparent. Even for the more modest values $N=0.2, C=50$ and $N=0.1, C=10$ shown in frames (c) and (d), the spectra retain distinctive profiles. We have found, however, that the dispersive profiles are less robust to the value of η than the hole burning profiles we consider next.

We now turn to the case of $\Phi=0$. For this value of phase, the anomalous features in free-space take the form of hole burning at line center, as well as pimple structures and the vanishing of the central contribution. In Fig. 4 we plot the cavity resonance fluorescence spectral intensity at line-center as a function of the Rabi frequency Ω for various values of N and C. The minima are clearly present in each plot and we expect anomalous features to arise for all these parameter values. It is worth noting the different form of the minima in each case. Figure 5 shows the spectrum corresponding to each of the line center plots in Fig. 4. As expected, hole burning exists in all four plots. Remarkably, it not only per-

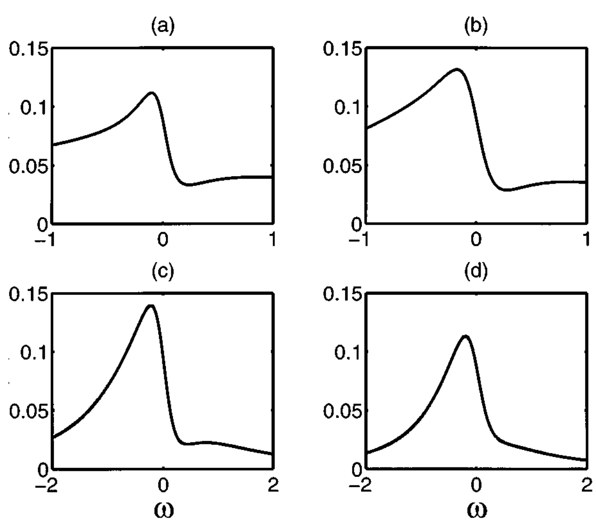

FIG. 3. The cavity resonance fluorescence spectra for $\Phi=\pi/2$ and (a) $N=1$, $C=125$, $\Omega=0.61$, (b) $N=0.5$, $C=100$, $\Omega=0.53$, (c) $N=0.2$, $C=50$, $\Omega=0.44$, and (d) $N=0.1$, $C=10$, $\Omega=0.33$.

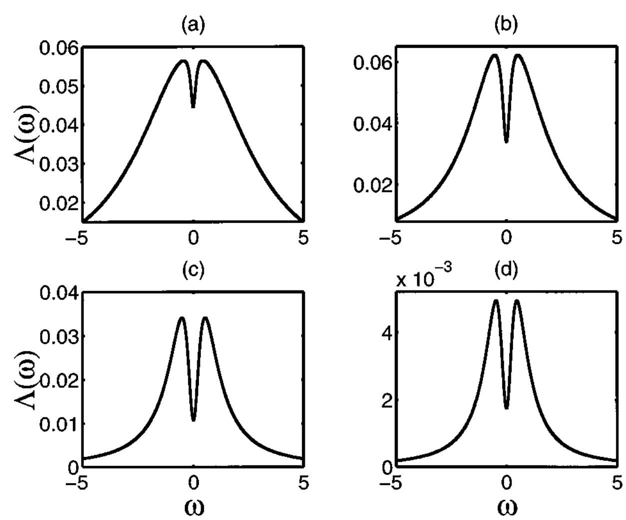

FIG. 5. The spectral plots for each of the cases in Fig. 4. Ω has been taken to be the minimum of the corresponding line-center plot.

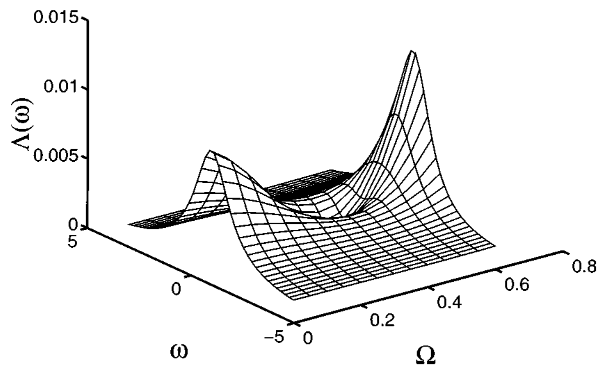

FIG. 6. A three-dimensional plot of the resonance fluorescence spectrum against Rabi frequency Ω for the case $N=0.01$, $C=10$, $\Phi=0$.

sists for very small values of N but it becomes even more pronounced as N is decreased (although obviously not for $N=0$), and perhaps more importantly, it persists for readily accessible values of C.

In Fig. 6 we present a three-dimensional (3D) mesh plot of the spectrum against Ω for $N=0.01, \Phi=0$, $C=100$, which shows the transition from normal to anomalous spectra, and then back to normal spectra again, as Ω is swept. The hole burning region is clearly visible and should be robust enough as a function of Ω to be observable in some of the cavity geometries presently in operation.

Figure 7 shows the 3D dependence of the spectrum at line center as a function Ω and Φ for $N=1$ and $C=100$. This reinforces what had already been indicated [16], that $\Lambda(0)$ possesses a minimum with respect to Ω only for smaller values of the phase, and consequently anomalous spectra do not occur for $\Phi \simeq \pi$.

Our considerations of the anomalous spectra have shown that, while some of the features predicted from our free atom analysis transpire to be too fragile to persist in this model (at least for practical parameter values) many of the interesting features have survived and are perhaps robust enough to be observed. Observation of such spectra would provide an unambiguous manifestation of the distinctive properties of the squeezed vacuum.

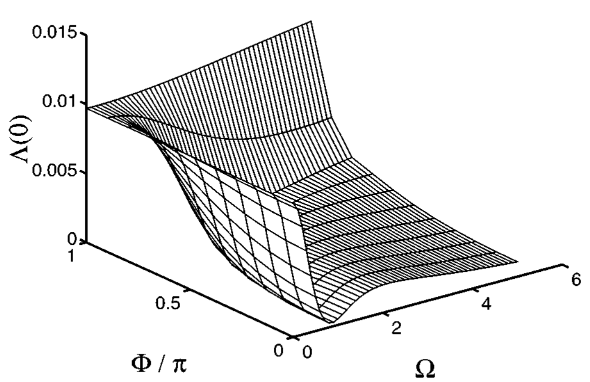

FIG. 7. A three-dimensional plot of the resonance fluorescence intensity at line center against Φ and Ω for the case $N=1$ and $C=100$.

IV. PURE STATES

We now consider another interesting effect that we found to coincide with the anomalous spectra. This is the collapse of the atom into a pure state. The first predictions of decay into a pure state in squeezed-light–atom interactions were made by Palma and Knight [19]. They considered a pair of two-level atoms damped by their interaction with a squeezed vacuum in the absence of a driving field. The equivalent three-level system was studied by Buzek, Knight, and Kudryavtsev [27]. Agarwal and Puri [20] considered a driven ensemble of two-level atoms in a squeezed vacuum and indicated the existence of special parameters values that lead to the decay into a pure state for the cases $\Phi=0$ and π.

Further considerations were presented for the single-atom case [21] by Tucci, who discussed this phenomenon from the point of view of the entropy of the system. He showed that for $\Phi=0$ the pure state achieved was an eigenstate of the σ_y Pauli operator. In [16] an in-depth analysis of the conditions for anomalous spectra was presented and shown to coincide with the condition for the atom to collapse into a pure state as well as the condition for amplification of a probe beam tuned to center frequency. The connection between these phenomena was clearly established and for $N \gg 1$ the expressions showed remarkable agreement. In fact even for $N \approx 1$ numerical evaluation of the complete expressions firmly justified the approximation made.

It was also pointed out that in the case $\Phi=0$ with $N \gg 1$ and $\eta=1$ an exactly pure state was achievable. For other phase values the atomic steady-state could only approximate a pure state.

There are several approaches useful in investigating the steady-state atomic purity. A convenient way, with the expressions we have already derived, is to consider the relationship between the steady state density matrix elements.

For any system,

$$\mathrm{Tr}(\rho^2) \leqslant 1, \tag{34}$$

and for a two-level atom this yields the simple condition

$$\rho_{00}\rho_{11} \geqslant |\rho_{01}|^2, \tag{35}$$

with equality being the condition for purity. Setting $\Phi=0$ and working in units of γ_c the condition for purity reduces to finding the zeros of the following expression:

$$\frac{1}{4}\Omega^4 + \frac{1}{2}\Omega^2[(2N_c+1)(N_c+\tfrac{1}{2}-M_c)-\tfrac{1}{8}]+N_c(N_c+1) \times (N_c+\tfrac{1}{2}-M_c)^2. \tag{36}$$

This expression, as a function of Ω, becomes identically zero only in the limit $N_c \gg 1$ and $\eta_c=1$ in which case $N_c+\frac{1}{2}-M_c$ vanishes, yielding $\Omega^2=1/4$. This was the condition mentioned in the free-atom analysis of [16,18]. However, as has been shown above, $\eta_c=1$ is not possible for

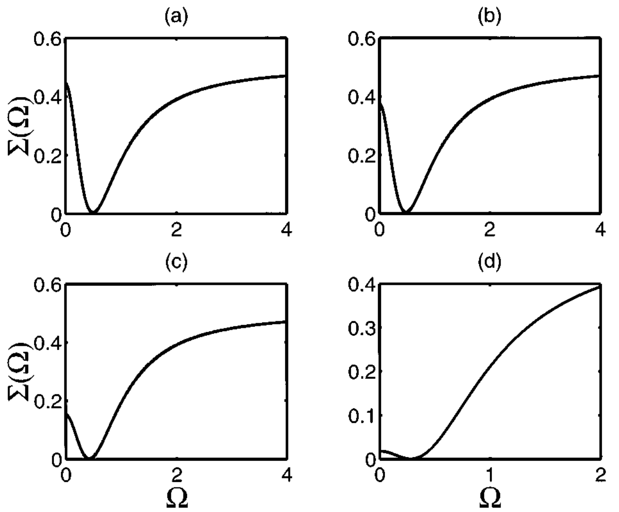

FIG. 8. The plot of the steady-state atomic purity $\Sigma=1-\mathrm{Tr}\rho^2$ against Ω for the same parameter values as Fig. 4. $\Sigma=0$ corresponds to a pure state.

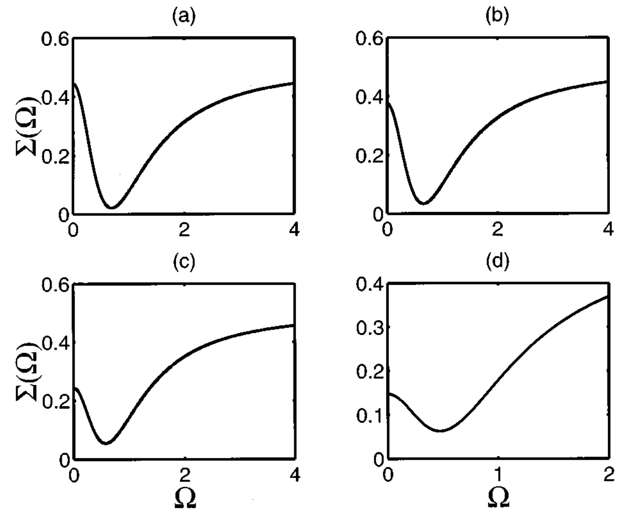

FIG. 9. The plot of $\Sigma=1-\mathrm{Tr}\rho^2$ against Ω for the same parameter values as Fig. 3.

finite C and consequently an exactly pure state is not achievable in this bad cavity limit. Having said this, we show that when these anomalous spectra do arise in our cavity model the dynamical equilibrium state of the atom is very well approximated by a pure state. That a quantum system can, via interaction with a reservoir, achieve what is very nearly a pure state is certainly surprising at least from the general perception of the role of standard reservoirs. This again is further demonstration of the nonstandard properties of a squeezed reservoir.

In Fig. 8 we plot $1-\mathrm{Tr}(\rho^2)$ as a function of the Rabi frequency Ω for the same parameter values as in Fig. 3. The coincidence of the minimum in each case with its equivalent case in Fig. 3 is apparent, the form of the curves around the minimum are also similar. It can be seen that as N is decreased, there is a slight discrepancy between the value of Ω which minimizes the line-center amplitude and that which maximizes the atomic state purity. In the free-space analysis of [16,18], for $\Phi=0$ and $N\gg1$, these two phenomena are optimized for the same value of Ω. Only for $\Phi=0$ may the atom be prepared in an exact pure state. We do not consider this case further here because we are concerned in remaining in that region of parameter space that is experimentally accessible.

In Fig. 9 we change the value of the phase Φ to $\pi/2$. The minimum in each plot is again clear, as is its approximate coincidence with the anomalous region depicted in Fig. 3, but what is also clear and consistent with our previous analysis is that the steady state achieved is less pure than for smaller phase values. Finally in Fig. 10 we show a 3D mesh plot of the atomic purity against Ω and Φ. This figure bears a striking resemblance to Fig. 7 from the point of view of indicating the existence of the particular parameter range over which the anomalous features can be expected and equivalently where the atom has evolved into what is very nearly a pure state. The two plots differ quantitatively in the central region and on towards the larger values of Ω . However, this is to be expected, in that as we move away from the anomalous region, the steady state of the atom is a more highly mixed state.

V. CONCLUSION

We have considered the resonance fluorescence spectra of a driven, cavity contained, two-level atom damped both by decay into the unsqueezed modes out the sides of the cavity and through the dissipation of the cavity field through the leaky output mirror, with a squeezed vacuum coupled to the system.

In the bad cavity limit we have shown the evolution equations for the atomic observables to be formally identical to those for the equivalent system in free-space, with the replacement of the actual squeezing parameters by effective squeezing parameters. We have also shown that some of the anomalous features in resonance fluorescence predicted for the free atom situation do in fact carry over to the cavity

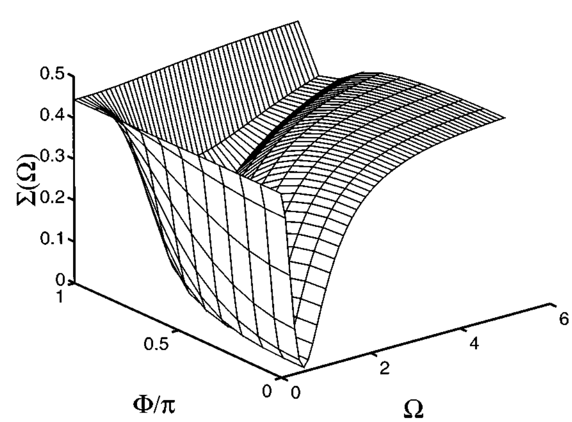

FIG. 10. Three-dimensional plot of atomic purity against Φ and Ω for the same parameter values as Fig. 7.

configuration and may be robust enough to permit observation.

When Rice and Pedrotti [24] considered this model they pointed out that it was quite a practical model for the observation of some predictions that had originally stipulated a 4π solid angle of squeezing. We feel that it would be a good candidate for the observation of the anomalous spectra, thereby providing further verification of the unique properties of the squeezed vacuum. Equivalently this could be viewed as a way of preparing an atomic system in what would be, for the correct choice of parameter values, very nearly a pure state. Thus it may be a practicable device for the investigation of various conjectures associated with Schrödinger catlike states.

ACKNOWLEDGMENTS

We wish to acknowledge helpful conversations with B.J. Dalton, Z. Ficek, and T.A.B. Kennedy. This research was supported by a NATO Collaborative Research Grant and by grants from the United Kingdom EPSRC and the EC. W.S.S. would also like to thank the Department of Education for Northern Ireland for financial support.

[1] V. Weisskopf, Ann. Phys. (N.Y.) **9**, 23 (1931).
[2] B. R. Mollow, Phys. Rev. **188**, 1969 (1969).
[3] F. Schuda, C. R. Stroud, and M. Hercher, J. Phys. B **7,** L198 (1974); W. Hartig,W. Rasmussen, R. Schieder, and H. Walther, Z. Phys. A **278**, 205 (1976); F. Y. Wu, R. E. Grove, and S. Ezekiel, Phys. Rev. Lett. **35**, 1426 (1975).
[4] H. J. Carmichael and D. F. Walls, J. Phys. B **9**, 1199 (1976); D. F. Walls and P. Zoller, Phys. Rev. Lett. **47**, 709 (1981); H. J. Kimble, M. Dagenais, and L. Mandel, *ibid.* **39**, 691 (1977); Phys. Rev. A **18**, 201 (1978).
[5] For reviews see, e.g., R. Loudon and P. L. Knight, J. Mod. Opt. **34**, 709 (1987); K. Zaheer and M. S. Zubairy, Adv. At. Mol. Opt. Phys. **28**, 143 (1990).
[6] H. P. Yuen and J. H. Shapiro, IEEE Trans. Inf. Theory **24**, 657 (1977); **26**, 78 (1980).
[7] C. M. Caves, Phys. Rev. Lett. **45**, 75 (1980).
[8] E. S. Polzik, J. Carri, and H. J. Kimble, Phys. Rev. Lett. **68**, 3020 (1992).
[9] R. E. Slusher, L. W. Hollberg, B. Yurke, J. C. Metz, and J. F. Valley, Phys. Rev. Lett. **55**, 2409 (1985).
[10] C. W. Gardiner, Phys. Rev. Lett. **56**, 1917 (1986).
[11] H. J. Carmichael, A. S. Lane, and D. F. Walls, Phys. Rev. Lett. **58,** 2539 (1987); J. Mod. Opt. **34**, 821 (1987).
[12] P. Goy, J. M. Raimond, M. Gross, and S. Haroche, Phys. Rev. Lett. **50**, 1903 (1983); W. Jhe, A. Anderson, E. A. Hinds, D. Meschede, L. Moi, and S. Haroche, *ibid.* **58**, 666 (1987); R. G. Hulet, E. S. Hilfer, and D. Kleppner, *ibid.* **55**, 2137 (1985); D. P. O'Brien, P. Meystre, and H. Walther, Adv. At. Mol. Phys. **21**, 1 (1985).
[13] J. J. Sanchez-Mondragon, N. B. Narozhny, and J. H. Eberly, Phys. Rev. Lett. **51**, 550 (1983); G. S. Agarwal, *ibid.* **53**, 1732 (1984).
[14] M. G. Raizen, R. J. Thompson, R. J. Brecha, H. J. Kimble, and H. J. Carmichael, Phys. Rev. Lett. **63**, 240 (1989); R. J. Thompson, G. Rempe, and H. J. Kimble, *ibid.* **68**, 1132 (1992); F. Bernadot, P. Nussenzveig, M. Brune, J. M. Raimond, and S. Haroche, Europhys. Lett. **17**, 33 (1992).
[15] A. S. Parkins and C. W. Gardiner, Phys. Rev. A **40**, 3796 (1989).
[16] S. Smart and S. Swain, Phys. Rev. A **48**, R50 (1993); Z. Ficek, W. S. Smyth, and S. Swain, Opt. Commun. **110**, 555 (1994); S. Swain, Phys. Rev. Lett. **73**, 1493 (1994).
[17] W. S. Smyth and S. Swain, Opt. Commun. **122**, 91 (1994).
[18] S. Swain and Peng Zhou, Phys. Rev. A **52**, 4845 (1995).
[19] G. M. Palma and P. L. Knight, Phys. Rev. A **39**, 1962 (1989).
[20] G. S. Agarwal and R. R. Puri, Phys. Rev. A **41,** 3782 (1990).
[21] R. R. Tucci, Int. J. Mod. Phys. B **5**, 1457 (1991).
[22] P. R. Rice and H. J. Carmichael, IEEE J. Quantum. Electron. **24** , 1351 (1988).
[23] H. J. Carmichael, R. J. Brecha, and P. R. Rice, Opt Commun. **82**, 73 (1991).
[24] P. R. Rice and L. M. Pedrotti, J. Opt. Soc. Am. B **9**, 2008 (1992).
[25] C. M. Savage, Phys. Rev. Lett. **60**, 1828 (1988); M. Lindberg and C. M. Savage, Phys. Rev. A **38**, 5182 (1988).
[26] S. Swain, Adv. At. Mol. Opt. Phys. **32**, 345 (1992), (1994); S. Smart and S. Swain, Phys. Rev. A **45,** 6857 (1992); **45**, 6863 (1992).
[27] V. Buzek, P. L. Knight, and I. K. Kudryavtsev, Phys. Rev. A **44**, 1931 (1991).